Journal of Colloid and Interface Science 566 (2020) 463–472

Contents lists available at ScienceDirect

Journal of Colloid and Interface Science

journal homepage: www.elsevier.com/locate/jcis

Facile synthesis of paper based graphene electrodes for point of care devices: A double stranded DNA (dsDNA) biosensor

J. Mohanraj [a], D. Durgalakshmi [a,*], R. Ajay Rakkesh [b], S. Balakumar [c], Saravanan Rajendran [d], Hassan Karimi-Maleh [e,f,g,*]

[a] Department of Medical Physics, CEG Campus, Anna University, Chennai 600 025, India
[b] CAS in Crystallography, Guindy Campus, University of Madras, Chennai 600 025, India
[c] National Centre for Nanoscience and Nanotechnology, Guindy Campus, University of Madras, Chennai 600 025, India
[d] Faculty of Engineering, Department of Mechanical Engineering, University of Tarapaca, Avda. General Velasquez, 1775 Arica, Chile
[e] School of Resources and Enviroment, University of Electronic Science and Technology of China, P.O. Box 611731, Xiyuan Ave, Chengdu, PR China
[f] Laboratory of Nanotechnology, Department of Chemical Engineering, Quchan University of Technology, Quchan 94771-67335, Iran
[g] Department of Applied Chemistry, University of Johannesburg, Johannesburg 17011, South Africa

GRAPHICAL ABSTRACT

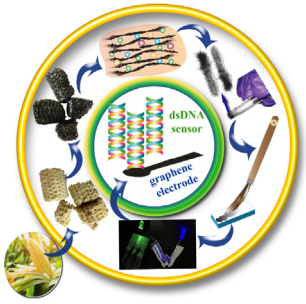

ARTICLE INFO

Article history:
Received 12 November 2019
Revised 23 January 2020
Accepted 23 January 2020
Available online 27 January 2020

Keywords:
Biomass
Graphene
Electrochemical
DNA
Sensor

ABSTRACT

The demand for high-quality graphene for electronic applications is increasing due to its high carrier mobility and electrical conductivity. In this connection, printing technology is a reliable method towards the fabrication of conductive, disposable graphene-based electrode for low-cost sensor application. Herein, we aimed to report the synthesis of high-quality graphene nanosheets obtained by electrochemical exfoliation of biomass-derived from corn cob. The conductive ink was prepared from this exfoliated graphene and was utilized for the preparation of paper-based graphene electrode towards double stranded DNA (dsDNA) sensor application. This paper, based graphene electrode opens the possibility of direct electrochemical analysis of analyte without any sample preparation. In this study, two irreversible oxide peaks were obtained from paper-based printed graphene electrode, corresponds to oxidation of guanine (G) and adenine (A) of dsDNA in the linear range of 0.2 pg mL^{-1} to 5 pg mL^{-1} with the detection limit of 0.68 pg mL^{-1} and the sensitivity of 0.00656 mA pg^{-1} cm^{-2}. Further, a small-scale printable circuit is fabricated using this graphene shows good conductivity of $1.145x10^{3}$(S/m).

* Corresponding authors at: School of Resources and Enviroment, University of Electronic Science and Technology of China, P.O. Box 611731, Xiyuan Ave, Chengdu, PR China (H. Karimi-Maleh) and Department of Medical Physics, CEG Campus, Anna University, Chennai 600 025, India (D. Durgalakshmi).
E-mail addresses: durgaklakshmi@gmail.com (D. Durgalakshmi), hassan@uestc.edu.cn (H. Karimi-Maleh).

https://doi.org/10.1016/j.jcis.2020.01.089
0021-9797/

1. Introduction

New type of nanomaterials and nanocomposite with amazing new properties created a great revolution in science [1–5]. Wide range application of nanoparticles and nanocomposites confirms their unique and interesting properties [5–10] Graphene, a first-ever discovered 2D crystalline material comprised of single-layer carbon atoms, which holds great attention and efforts in the field of material science [11,12]. This material reveals numerous leading potential applicable ventures. Graphene has higher magnitude of crystallinity, tunable bandgap possibility and possesses a multi-functional property of electronic [13–16], mechanical [17–19], optical [20–23] thermal[24–27], and biocompatibility[28–31], signifies this material as a promising candidate for nanoelectronic devices [32,33].This phenomenal material also paves way in fascinating towards the fabrication of paper based electrode for energy storage devices[34–37], and have remarkable potential for direct electrochemical analysis of bio-fluids like blood [38–40], saliva [41,42], and urine[43–46]. Among the several early-stage screening techniques, electroanalytical detection has more attention owing to its direct analysis and ease of use [47], handheld size, and specific fields like clinical diagnostics, bioremediation, environmental monitoring and controlling the food quality without any sample preparation. Unlike the conventional methods (e.g. using substrates of glass, ceramic and polymer) these paper-based biosensors exhibits several advantages such as affordable, biocompatibility, biodegradable, high abundance, and disposable [48–54]. Typical fabrication techniques for paper-based biosensor such as photolithography [55–57] wax printing [57,58], screen printing [57,59] and inkjet printing [58,60–62] are recent trends. In spite of this, the essential of disposable electrochemical sensor is expected to offer a measurable signal quantitatively and qualitatively at a stipulated time. Hence, in the coming years ahead, this printed electrode will be an economically affordable and disposable with a precise analytical testing tool that is technologically applicable in the future.

DNA sensing by electrochemical method is most important evolving technique in recent days. It is used to detect the existence of pathogenic micro-organisms and DNA damage in various types of cells [63–66]. Furthermore, DNA sensor is used for the determination of individual concentration of adenine (A) and Guanine (G) and estimation of their ratio in nucleic acid [67]. Whilst the catabolism of nucleic acids, enzymatic degradation of tissues, dietary habits and various salvage pathways can be estimated from the biosensor signals obtained from the physiological fluids, tissues, and cells, that could be an indicative tool and used to detect certain diseases [68,69]. So far, an earlier conventional method of DNA sensors consists of labeling with fluorescent dyes and radioactive tags along with some enzymes. This has been employed to tailor the optical properties to ensure the hybridized DNA from targeted single-stranded DNA [70].There are only few reports available based on Double standard deoxyribonucleic acid(dsDNA) electrochemical sensors. Earlier, it has been reported on the detection of dsDNA against anticancer derivative of quinalozine using SPCE and MWNT/SPCE electrode [71]. And also, ionic liquid modified screen-printed graphite electrode for direct electrochemical detection of dsDNA has also been reported by J. Ping *et al.* [72]. Lenka Hlavata et al. studied on screen-printed carbon electrode for direct electrochemical detection of DNA damage against UV-C radiation and chemical agents [73]. Recently, Zhihoing Zhu et al., examined the ordered mesoporous carbon modified carbon ionic liquid electrode for direct electrochemical detection of dsDNA in the range of 10–600 μg mL^{-1} by differential pulse Voltammetry (DPV) with the detection of 1.2 μg mL^{-1} [74]. Dongyang Wang and co-workers studied Cu@Ni/MWNTs nanocomposite for simultaneous electrochemical determination of guanine and adenine in the range of 1.0–180 μM and 2.0–150 μM by cyclic Voltammetry (CV). From these earlier reports it can be noted that the electrochemical detection for dsDNA has proved to be reliable and also required the least amount of sample for analysis by cyclic Voltammetry and Differential pulse Voltammetry electroanalytical method [75].

High quality and mass production of graphene is essential with an affordable low cost are essential for large scale electronic and sensing applications. The commercially available graphite taken as starting material for the production graphene can be a good choice but it is polluting the environment during treating with an oxidative chemical. To overcome this, biomass-derived graphene significantly offers a novel, low cost, environmentally friendly, with the carbon-rich functional material. Biomass corn cob was made up of ~40 wt% of carbon content and very low trace elements (1.5 wt%) was reported [76,77]. Among several synthesis methods of graphene [78–83], electrochemical exfoliation [82,84–86] is an effective method compared to that of conventional synthesis method like chemical vapor deposition (CVD) [87–89] and Hummers method [90–92]. However, the electrochemical exfoliation of graphene from biomass is not yet reported, that we achieved for the first time.

Herein we report, on the investigation of label-free, low-cost graphene-based biochar exfoliated graphene nanosheets and fabrication of paper-based electrode for electrochemical analysis of calf thymus double standard DNA. This paper-based electrode shows an expected direct electrocatalytic oxidation of dsDNA with lower overpotential compared to that of commercially available glassy carbon electrode, which can be replaceable in forthcoming years. In electrochemical sensing, the parameters such as concentration and potential were fixed for the determination of dsDNA using paper-based graphene electrode, and this can be used for direct analysis of human excretory metabolites like serum, urine, sweat, and saliva in the future.

2. Experimental

2.1. Reagents and equipment

Sodium sulfate (99%), Hydrochloric acid (A R grade), and calf thymus DNA were procured from Alfa Aesar, respectively. In house prepared graphite was used as a precursor for graphene preparation. DC power supply (Pico, India) was used to exfoliate the graphene from biochar graphite obtained from corn cob. Raman spectroscopy (LabRAM-Laser wavelength-488 nm, France) was used to investigate the formation of graphene, FT-IR spectroscopy (Jasco FT/IR- 6600, USA) was used to record the spectra in the range from 4000 cm^{-1} to 400 cm^{-1} to confirm the functional group's presence in the graphene. X-ray diffraction (XRD) data were collected from using PANalytical X-ray diffractometer utilizing Cu Kα (λ = 1.54Å) radiation. The samples were scanned in the 2θ range from 10° to 60° and all of the peaks were assigned and confirmed with the published database by the Joint Committee on Powder Diffraction Standards (JCPDS). The morphology of the samples has been examined using Scanning Electron Microscopy (Hitachi-N3400, Singapore). High-resolution scanning transmission electron microscopy (HRTEM, JEOL JEM 2100) analysis was carried out to understand the layered structure of the graphene. Surface area and pore size distribution analysis were studied using BelsorpMicrotrac mini-II. Studies on I-V Characteristics were analyzed using four-probe method (Hitech ceramics, India). Cyclic voltammetric measurement (DNA sensor) has been acquired using SP-300 (Biologic, France).

2.2. Preparation of graphene by electrochemical technique

Electrochemical exfoliation of graphene from biochar graphite was achieved by two-electrode system, utilizing biochar corn cob fixed with graphite pencil (HB writing grade) as the working electrode (anode) and stainless-steel plate of 2 cm X 1 cm as the counter electrode (cathode). The scheme of exfoliation procedure is depicted in Fig. 1a. There are several types of aqueous inorganic salts solutions used as electrolytes for exfoliation. Amongst them, sulfate compound of Na_2SO_4 reveals good exfoliation ability reported by Parvez *et al.* and Chuang *et al.* [84,93]. Briefly, 0.5 M concentration of Na_2SO_4 (7.102 g) salt was dissolved in 100 mL of double-distilled water (DDH_2O), the result electrolyte solution pH value was measured as ~7.0. During the electrochemical process, the distance between the counter electrode and working electrode was kept at a constant value of 2 cm. A DC potential of 20 V was applied to the working electrode after dipping into the electrolyte solution. Water bubbles originated at the biochar derived corn cob graphite at cathode evidence the exfoliation of graphene from graphitic layers. When the bias voltage is applied at the cathode, it causes oxidation of water, result in the production of a strong nucleophile hydroxyl ion (OH^-). An anion attack take place on the edge sites followed by grain boundaries of graphite and the depolarization at these sites lead to the intercalation of sulfate ions in between the graphite layers. This is due to low electrochemical reduction potential of an electrolyte containing sulfate (SO_4^{2-}) anions and self-oxidation of water, which could be favored for generating gaseous species of SO_2 along with O_2. However, such a gaseous species are responsible for rapid exfoliation graphene sheets within few minutes and hence it shows a good exfoliation efficiency [94]. For instance, in the same solution sequence of electrochemical experiments, ~2.7 g of graphene sheets was yielded within 45 min. The obtained graphene sheets were washed with concentrated HCl to eliminate the impurities, followed by dried and calcinated in the presence of an inert gas atmosphere. In order to increase the exfoliation rate a wash dried graphene sample was further probe sonicated (Fig. 1b) in the presence of acetone and water in the ratio of 3:1 for 2 h in optimized parameters (e.g. Sonication time 40 s, interval gap 20 s, power density 60%, and maintained temperature is 45) [95].The samples were termed as graphite, as prepared graphene (Gasp), graphene wash dried (GWD), graphene without wash (GWOI), graphene washed (GWI) with calcination in inert gas, and graphene probe sonication (GPS), respectively.

2.3. Fabrication of graphene-based paper electrode

In order to fabricate electrodes from the synthesized graphene, 15 mg of exfoliated graphene (GWI and GPS) were mixed with a few drops of commercial transparent polyvinyl acetate solution using a vortex mixer for about 5 min and transferred to Petri dish. The obtained conductive graphene paint to draw a specific structure, the paint brush pen is soaked well with conductive paint in the paint container, and these paints are transferred to the paper substrate (commercial A4-100 GSM sheet) under required hand pressure. This as-prepared conductive paper is further dried at 150 °C for 2 h in the oven to prevent from graphene peel off from the paper substrate. The stepwise procedure for the preparation of paper-based graphene electrode is shown schematically in Fig. 1c.

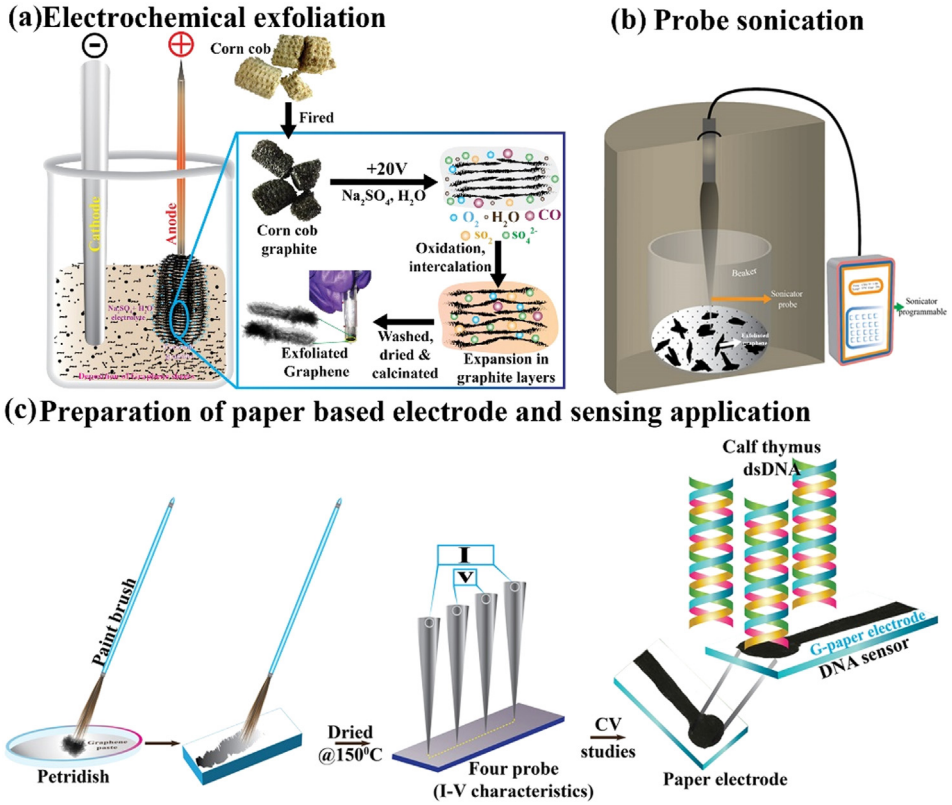

Fig. 1. Schematic representation of (a) electrochemical exfoliation of graphene sheets from corn cob (e.g. when applied 20 V potential into corn cob graphite electrode which intercalated, expanded and exfoliated in the presence of sulphate ions, as a result, biochar exfoliated graphene nanosheets were obtained). (b) Probe sonication process is conducted by optimized parameters such as sonicating time interval and temperature; and (c) Fabrication of paper-based graphene electrode using polyvinyl acetate solution mixed with graphene in petridish, resultant will be graphene paint and that was painted on the paper substrate. After drying, the electrical conductivity painted graphene electrode have been examined using four probe method and further used as dsDNA biosensor.

2.4. Preparation of dsDNA for electrochemical cyclic voltammetry sensing

Calf thymus dsDNA was procured from the SRL, India. Form this, stock concentration of 2 mg /2mL was prepared in PBS solution (pH = 7.4) and in double-distilled water. Nonetheless, form the stock solution it was further diluted in PBS and water and these solutions were used for dsDNA sensing by electrochemical analysis.

2.5. Voltammetric and impedimetric detection procedure

The analysis all the voltammetric studies were examined in the presence of phosphate buffer solution (PBS) (pH = 7.4) and double distilled water (DDH_2O) associated with the final concentrations from 10pL to 10nL of dsDNA. The cyclic voltammetric data were recorded in the range of ±10 V with the rate of scan at $100mVs^{-1}$. An impedance measurement was carried out in the range of 50 kHz to 0.05 Hz, with a sinusoidal voltage interval of 10 mV amplitude. All of these studies were recorded in the same electrolyte without any redox marker except PBS. The acquired impedances spectra were further analyzed using Nyquist plots ($-Z_i$ vs, Z_r) by their relative fitted impedance spectra represented via equivalent circuit. The goodness of the fit was acquired from chi-square value using Z-fit software.

3. Results and discussion

3.1. Studies on Raman spectroscopy

The excitation laser source at 488 nm of Raman spectra of biomass corn cob derived exfoliating graphene is shown in Fig. 2(a) for Graphite, GPS, Gasp, GWD, GWOI, and GWI, respectively. In the exfoliated graphene Raman characteristic band was observed for D-band at1393 cm^{-1},1375 cm^{-1}, 1375 cm^{-1}, 1379 cm^{-1}, 1373 cm^{-1}, 1379 cm^{-1}, for graphite, GPS, Gasp, GWOI, GWD, and GWI, respectively. Similarly, the characteristic G-band was observed to be at 1621 cm^{-1}, 1596 cm^{-1}, 1592 cm^{-1}, 1596 cm^{-1}, 1589 cm^{-1}, 1596 cm^{-1}, for graphite, GPS, Gasp, GWOI, GWD, and GWI, respectively. And the 2D is at 2737 cm^{-1}, 2726 cm^{-1}, 2737 cm^{-1}, 2730 cm^{-1}, 2737 cm^{-1}, for GPS, Gasp, GWOI, GWD, and GWI, respectively [96]. The intensity of the disorder-induced D band (1375 cm^{-1}) is relatively lesser than that of G band (1596 cm^{-1}) for the exfoliated samples. This is due to the highly ordered magnitude of carbon atoms; from this it is also observed the I_D/I_G ratio decreases eventually with respect to graphite. The 2D band is the clear evidence on the occurrence of few layers of graphene which is shown in Fig. 2(b-f). The 2D band was originated from a two-phonon double resonance Raman process and it is a closely related band structure of graphene layers. However, the deconvolution of 2D bands and their relative intensities of I_{2D}/ I_G ratio (0.27, 0.22, 0.22, 0.21 and 0.22 for GPS, Gasp, GWOI, GWD, and GWI, respectively) indicates the presence of bilayer to four layers of graphene from Gaussian fitting. Thus 2D band has merely been of approximately bilayer graphene for GWI and GPS and this result is comparable with the TEM images [97]. Further deconvoluted Raman spectra evidences that the bilayer to four layers of graphene and the fitted peaks for GPS, Gasp, GWOI, GWD, and GWI has shown respectively four, two, four, five, four peaks with fitted $\chi 2 \cong 1$. Further the average crystallite size of sp^2 domain L_a(nm) in the graphene nanosheets using intensity ratio $I_D'I_G$ was calculated by T and K correlations given in Eq. (1) [98].

$$L_a(nm) = \left[2.4 * 10^{-10}\lambda_L^4\right]\left[\frac{I_D}{I_G}\right]^{-1} \quad (1)$$

where, λ_L is the Laser excitation wavelength (488 nm) and an I_D/ I_G is corresponding to Intensity ratio of D band and G band ratio of graphene. The calculated crystallite size (L_a) is 23.09 nm, 37.80 nm,

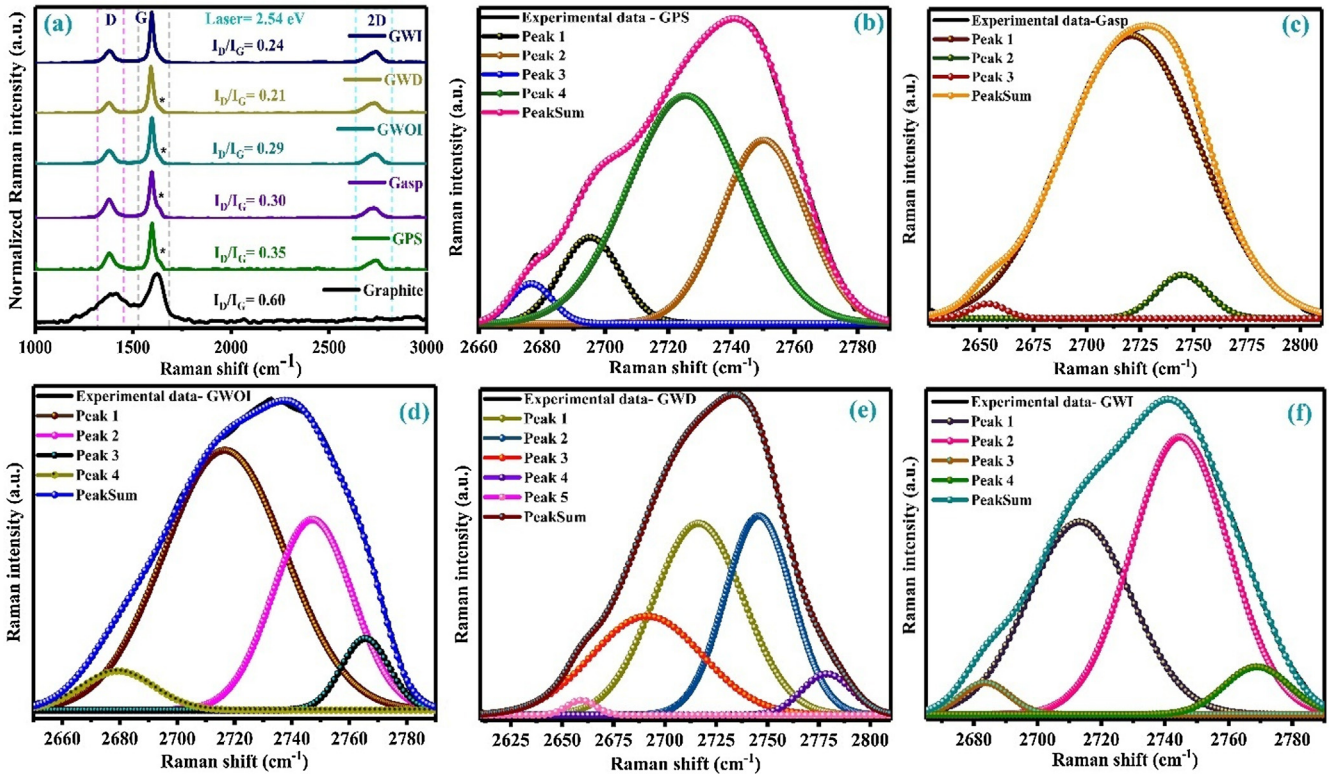

Fig. 2. Raman spectrum (laser-488 nm) of (a) graphene structures obtained from corn cob derived exfoliated graphene with respective I_D/ I_G for graphite, GPS, Gasp, GWOI, GWD, GWI and their corresponding Gaussian deconvoluted and fitted Raman spectrum (b to f) is evident of few layers of graphene nanosheets.

45.36 nm, 46.93 nm, 59.56 nm and 55.32 nm, for graphite, GPS, Gasp, GWOI, GWD, and GWI, respectively. The results exhibited that higher magnitude of sharp crystalline peak in Raman spectra which also compared with the sharp X-ray diffraction pattern.

3.2. Studies on the functional group, structural and porosity analysis

The FTIR spectrum is shown in Fig. 3(a) indicates the presence of some functional groups in the biomass corn cob derived graphene. The peak around 1588 cm^{-1}, 1033 cm^{-1}, 957 cm^{-1}, and 458 cm^{-1} are attributed to aromatic C=C stretching bond, C-O stretching vibration, Si-O vibration of stretching, and stretching vibration of Si-O-Si, respectively. To further confirm the formation of graphene from biomass corn cob, it was examined by XRD. The XRD pattern of GPS, Gasp, GWOI, GWD, and GWI graphene is shown in Fig. 3(b) and in Fig. S1 for graphite. All the prepared graphene has 002 lattice plane at 26.54°, which is well-matched with the JCPDS card no- 41-1487. In case of the Gasp and GWOI, graphene shows some impurities along with the shift towards lower angle, this might be due to the crystallized silica peak shown at 21.09°. There are no impurity peaks observed for GWD and GWI.

The quantitative surface area and porosity for exfoliated graphene-like GPS, GWI, and GWD were examined using BET nitrogen adsorption–desorption studies (Fig. 3c). The BET specific surface area was found to be 85.625 m^2/g, 69.072 m^2/g, and 61.379 m^2/g for GWD, GPS, and GWI, respectively. A lower value of specific surface area has been observed for GWI, which is expected to be in the range of standard mesoporous structure. Similarly, the nitrogen adsorption isotherm behavior was observed for the GWD, GPS, and GWI, and the pore diameter was obtained to be 5.4079 nm, 8.4155 nm, and 5.4136 nm, respectively.

3.3. Morphological analysis for biomass corn con derived exfoliated graphene

The morphology of the biomass corn cob derived graphene was examined by SEM and HRTEM. Fig. 4(a) shows the SEM image of the graphite with wrinkles and double gauze-like morphology at the border. This shows that graphene remains in its thermodynamically stable state, and in Fig. 4(b-f) the sheets like morphology for electrochemical exfoliation of biomass-derived graphene has been confirmed. The elemental composition for (a) graphite, (b) Gasp, (c) GWOI, (d) GWI, (e) GWD and (f) GPS from EDAX pattern is shown in Fig.S2 [93,99]. Fig. 4(g-h) is shown the HRTEM images of exfoliated graphene has bilayer to few layers of graphene which is in complement to the Raman deconvoluted data. The graphene sheet was also observed to be of larger dimension and without any defects proves the quality of the obtained graphene structure with the dimension for length, breadth, and thickness as ~7.70 μm, ~5.19 μm, and ~53.81 nm, respectively. The selected area electron diffraction (SAED) pattern exhibits the strong diffraction plane, which shows the high crystallinity of well-organized carbon atoms in the synthesized graphene. The six-fold hexagonal pattern with brighter diffraction spots and crystalline domain confirms the occurrence of graphene nanosheets. Further the observed multiple hexagonal patterns also evidence the presence of bilayer to few layers of graphene [100,101].

3.4. Cyclic Voltammetry studies of paper-based dsDNA sensor

All the prepared graphene (GWI, GPS, and GWD) based paper electrode was examined for cyclic Voltammetry analysis, shown in Fig. 5. Among these, the paper-based graphene electrode fabricated using GWI electrodes expected a dsDNA signal due to their lower in electrical resistance compared with that of other graphene (GPS and GWD) paper electrode. Fig. 5(a) revealed the typical cyclic voltammograms of paper-based graphene (GWI) electrode in the presence of different concentration of dsDNA in PBS solution. During the analysis, an increase in the concentration of dsDNA in PBS solution shows a linear increase in the peak current (Fig. 5d). The prepared paper-based graphene (GWI) electrodes prove a notable response to the cyclic voltammetric signal to dsDNA about + 1.07 V on the positive side, even in the range of lower concentration (0.2 pg/mL to 5 pg/mL) level. Additionally, the same electrochemical cyclic voltammetry analysis was carried out for all the preparation graphene (GWI, GPS, and GWD) based electrode at higher concentration of dsDNA (10pL). Fig. 5c depicts electrochemical signal of graphene (GWI) based paper electrode shows increasing in the current intensity along with peak broadening. This could be due to the redox potential of adenine, which is about +1.06 V with lower current compared to that of GWD, GPS and GC (e.g. glass carbon signals of G show at higher peak current at the inset of Fig. 5a. And another graphene (GPS and GWD) paper-based electrode has lower in peak current and broad in peak compared to graphene (GWI) based paper-based electrode. The lower redox potential and lower overpotential for the electrochemical oxidation of dsDNA were shown in Fig. 5 (b-c). Similar to the direct cyclic voltammetric detection of dsDNA in the presence of PBS solution, double distilled water (DDH_2O) was taken as another electrolyte. During the electrochemical sensing, decreasing in the peak current was observed with an increase in the concentration of dsDNA, shown in the Fig. S4 (supplementary information).

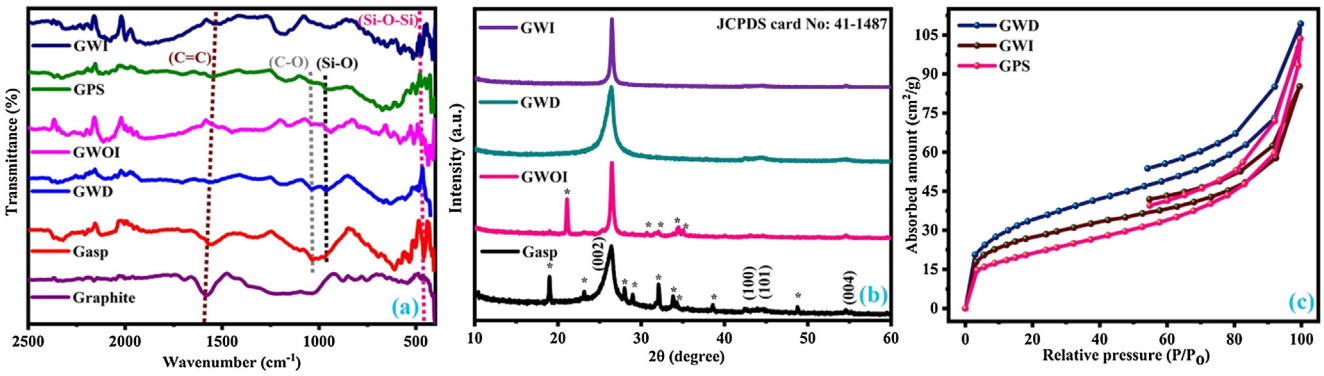

Fig. 3. (a) FTIR spectra for identification of carbon and oxygen functional groups in graphite, GPS, Gasp, GWOI, GWD, GWI, and (b) X-ray diffraction pattern with highly ordered crystalline graphene nanosheet. (c) analysis of porosity for GWD (5.4079 nm), GWI (8.4155 nm), and GPS (5.4136 nm) of biomass-derived corn cob exfoliated graphene using Brunauer-Emmett-Teller (BET) technique.

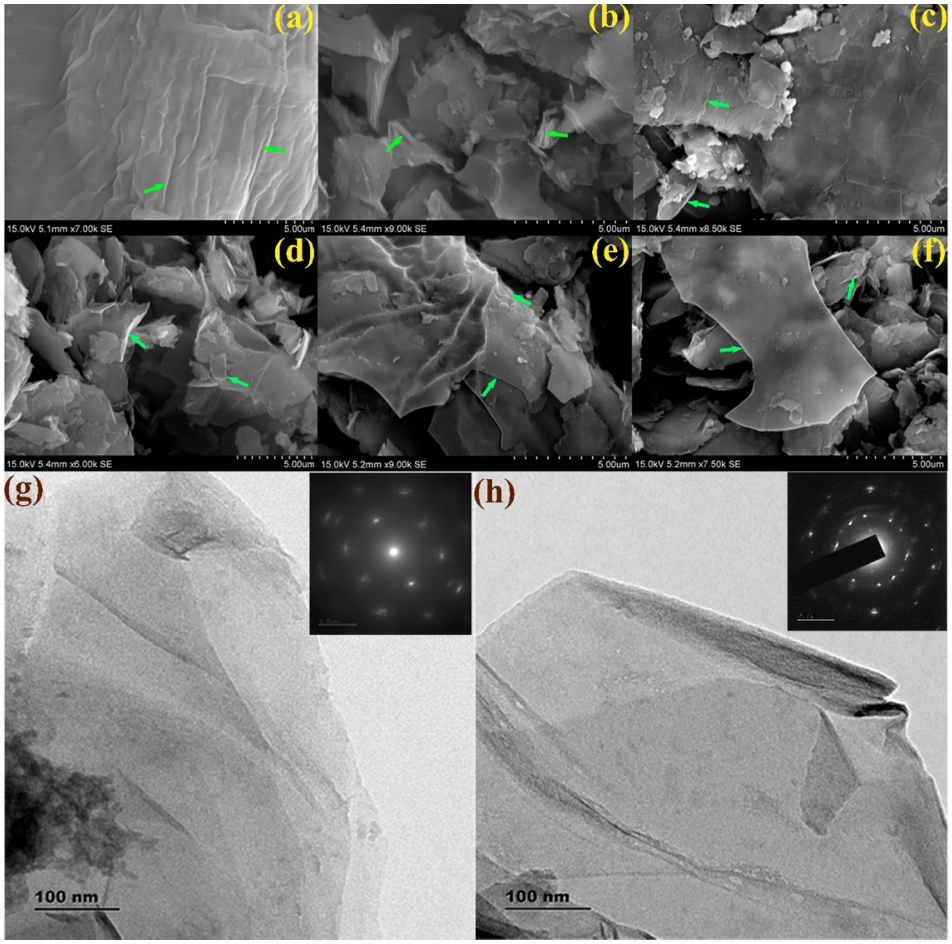

Fig. 4. SEM image of (a) graphite shows wrinkle structure on the surface. Surface morphology of (b) Gasp, (c) GWOI, (d) GWI, (e) GWD and (f) GPS shows large size exfoliated graphene nanosheets. HRTEM images of (g) GWI and (h) GPS shows few layers of graphene nanosheets without defect and highly ordered graphene nanosheet structure. (Inset image in g and h: SAED pattern is evident of highly crystalline of both GWI and GPS exfoliated graphene nanosheets).

3.5. Effect of concentration of dsDNA

The effect of dsDNA concentration subjected to the cyclic Voltammetry of dsDNA for paper-based graphene electrode was investigated and shown in Fig. 5(d). It can be seen that, with an increase in the concentration of dsDNA, there is a gradually increased in the peak currents. The linear relationship was calculated between the concentration of dsDNA and the peak current in the range of 0.2 pg/mL to 5 pg/mL. The linear regression, correlation coefficients of 0.9735 and the limit of detection was estimated to be 0.68 pg mL^{-1} and the sensitivity was calculated as 0.00656 mA pg^{-1} cm^{-2} using the Eq. (2) [102].

$$Sensivity = \frac{Slope\ \ of\ \ the\ \ calibration\ \ curve, m(mA\ \ pg^{-1})}{Active\ \ sensing\ \ area, A(cm^2)} \qquad (2)$$

In comparison to our present work, earlier work reported by Yang Fan et al on TiO_2-graphene nanocomposite exhibits dsDNA in the range of 0.5 μM-200 μM with the detection limit of 0.10 μM and 0.15 μM for adenine and guanine [101]. Jianfang Ping et al., fabricated an ionic liquid modified screen-printed electrode for direct electrochemical analysis of dsDNA in the range of 20 μg mL^{-1} to 120μgmL^{-1} with the detection limit of 5 μg mL^{-1} [72]. Zhinong Zhu et al., studied an ordered mesoporous carbon modified with ionic liquid for electrochemical analysis of dsDNA to the range of 10–600 μg $mL^{-1}$with the LOD of 1.2 μg mL^{-1} [74]. Emiliano N. Primo et al., reported the electrochemical detection of calf thymus dsDNA in the range of 0.25–2.50 × 10^{-3}M with the limit of 50 μM using bamboo like MWCNT [103]. And hence our prepared paper-based graphene electrode revealed the higher linear range and the limit of detection for the dsDNA at a low cost which has comparable results with above mentioned earlier work reports.

3.6. Impedimetric detection of dsDNA

Fig. 5(e-f) shows the Nyquist plots obtained from impedance analysis, and the corresponding Randels equivalent circuit was fitted to the experimental data. In the circuit, the parameter R_1 denotes the resistance of the solutions; R_2 represents to the resistance to the charge transfer between the solution and the electrode surface; R_3 corresponds to the resistance in between the electrode and paper substrate; $C_1$is associated to the sandwich between interface of electrode and electrolyte solution, which act as double-layer capacitance; $C_3$is attributed to the double-layer capacitance due to the interface between the printed electrode and the paper substrate. Taken together, we examined on the charge transfer resistance between the electrode surface and the solution and possible to find out each process step to target biomolecule. With increasing in the concentration of dsDNA increasing in impedimetric resistance is observed due to active graphene surface covered by of dsDNA sequential addition. The negatively charged phosphate group in the dsDNA skeleton, is responsible for the electrical repulsion results in increase in resistance. Fig. 5f depicts that, the highly negatively charged graphene probe sonication (GPS)

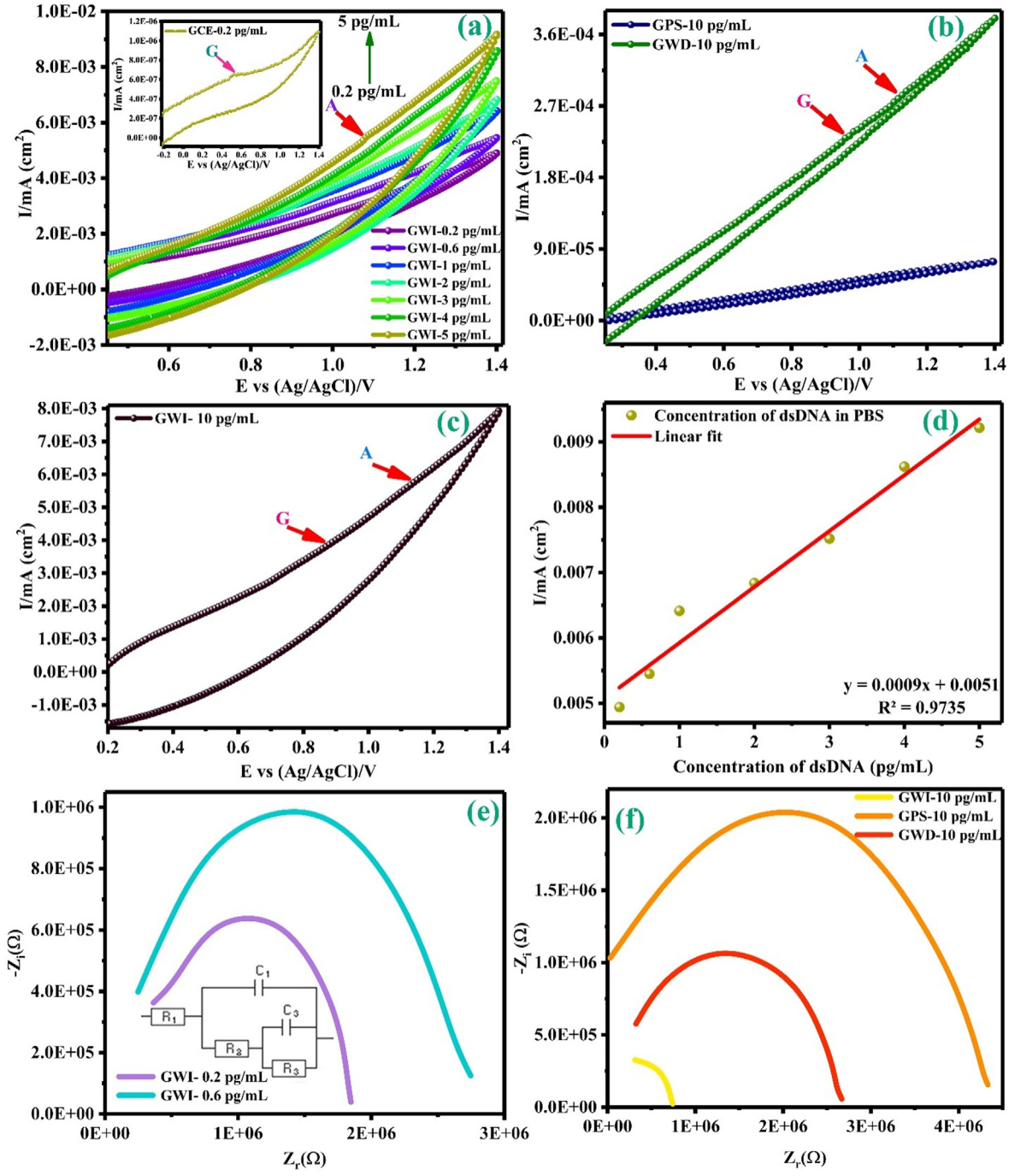

Fig. 5. The cyclic voltammograms and EIS spectra of paper-based graphene (GWI) electrode at (a) different concentration of dsDNA in PBS (Inset-cyclic voltammogram of bare glassy carbon electrode), (b &c) higher concentration of dsDNA signal response for various paper-based graphene (GPS, GWD, and GWI) electrode, (d) effect of dsDNA concentration in PBS solution with a linear fit for graphene paper-based electrode (GWI). (e) EIS response of various concentration to dsDNA for GWI based paper electrode, and (f) higher concentration of dsDNA signal response for various method of prepared paper-based graphene (GPS, GWD, and GWI) electrode.

shows higher inhibition of interfacial electron transfer rate compared to that of GWI and GWD.

3.7. Studies on electrical potential and stability measurement

In order to understand the electrical conductivity, LED conductivity test was performed on the GWI based graphene ink drawn on paper. There were no visible breakages in the circuit even after fold, bend, twist and provide flexibility to graphene painted on the paper. The LED were connected without any conductive paste and powered using a 9 V battery, cause bright light emission of Green and Blue at distinct folded sates shown in Fig. 6(a) and the conductivity characteristics of GPS based paper electrode is shown in supplementary Fig. S5. The electrical conductivity was measured with respect to the applied voltage using a four-probe resistivity setup. The electrical conductivity is increasing linearly from 5 V to 50 V and it obeys the ohm's law is shown in Fig. 6(b). The conductivity is calculated as 1.145×10^3(S/m) and it is comparable with earlier work of direct ink writing graphene electrode [104–107]. This result shows that, the paper-based graphene

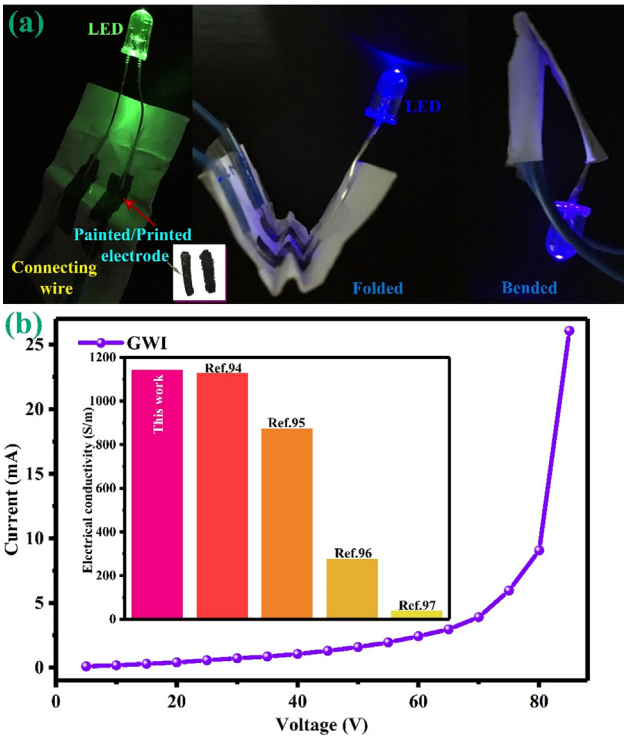

Fig. 6. Photograph of (a) LED lit-up step obtained using conductive biomass-derived electrochemical exfoliation of graphene-based paper electrode of GWI (Inset: photograph of paper electrode), (b) the electrical conductivity studies by I-V characteristics measurement for GWI paper electrode using the four-probe method.

electrode exhibits an efficient electrical conductivity, due to its highly ordered graphene structure. Further increasing the applied voltage drastically increasing in the current [108] which could be due to enabling the electrons flow by hop mechanism through the π-π conjugated carbon atoms.

4. Conclusion

In conclusion, high yield and high-quality graphene was obtained by electrochemical exfoliation of biomass-derived graphite. The obtained graphene nanosheets possess great potential for its use towards conductive graphene ink for fabricating paper-based electrode. The paper-based graphene electrode was employed for direct electrochemical analysis of dsDNA. An oxidative peak was obtained using paper-based graphene electrode which is corresponding to the oxidation of adenine (A) at lower overpotential which proves the response of electrochemical oxidation peak for dsDNA. The linear range was determined for the dsDNA from the range of 0.2 pg/mL to 5 pg/mL with the detection limit was estimated about 0.68 pg mL^{-1} with the sensitivity of 0.00656 μA pg^{-1} cm^{-2}. This study will be a stepping stone for producing paper-based sensor and printable circuits at affordable cost, environmentally friendly, disposable, and biodegradable in future.

CRediT authorship contribution statement

J. Mohanraj: Writing - review & editing. **D. Durgalakshmi:** Writing - original draft, Writing - review & editing. **R. Ajay Rakkesh:** Writing - original draft. **S. Balakumar:** Synthesis. **Saravanan Rajendran:** Writing - original draft. **Hassan Karimi-Maleh:** Sensor studies.

Declaration of Competing Interest

The authors declare that they have no known competing financial interests or personal relationships that could have appeared to influence the work reported in this paper.

Acknowledgement

The authors D. Durgalakshmi and J. Mohanraj gratefully acknowledges DST-INSPIRE Faculty Fellowship under the sanction DST/INSPIRE/04/2016/000845 for their funding. All the authors acknowledge DAE-BRNS - 2009/34/38/BRNS and DST-PURSE-9500/PD2/2014 for providing equipment facilities. The authors (S.R.) acknowledges the support of CONICYT through the project CONICYT/FONDAP/15110019 and FONDECYT Government of Chile (Project No.: 11170414).

Appendix A. Supplementary material

Supplementary data to this article can be found online at https://doi.org/10.1016/j.jcis.2020.01.089.

References

[1] S. Malekmohammadi, H. Hadadzadeh, S. Rezakhani, Z. Amirghofran, Design and synthesis of gatekeeper coated dendritic silica/titania mesoporous nanoparticles with sustained and controlled drug release properties for targeted synergetic chemo-sonodynamic therapy, ACS Biomater. Sci. Eng. 5 (2019) 4405–4415.
[2] N. Sabaghnia, M. Janmohammadi, M. Dalili, Z. Karimi, S. Rostamnia, Environ. Sci. Pollut. Res. 26 (2019) 11719–11729.
[3] E. Doustkhah, Y. Ide, Bursting exfoliation of a microporous layered silicate to three-dimensionally meso-microporous nanosheets for improved molecular recognition, ACS Appl. Nano Mater. 2 (2019) 7513–7520.
[4] S.I. Kaya, B. Demirkan, N.K. Bakirhan, E. Kuyuldar, S. Kurbanoglu, S.A. Ozkan, F. Sen, J. Pharm. Biomed. Anal. 174 (2019) 206–213.
[5] E. Hosseini, A. Rajaei, M. Tabatabaei, A. Mohsenifar, K. Jahanbin, Preparation of pickering flaxseed oil-in-water emulsion stabilized by chitosan-myristic acid nanogels and investigation of its oxidative stability in presence of clove essential oil as antioxidant, Food Biophys. (2019), https://doi.org/10.1007/s11483-019-09612-z.
[6] E. Doustkhah, A. Baghban, M.H.N. Assadi, R. Luque, S. Rostamnia, Catal. Lett. 149 (2019) 591–600.
[7] H. Karimi-Maleh, M. Shafieizadeh, M.A. Taher, F. Opoku, E.M. Kiarii, P.P. Govender, S. Ranjbari, M. Rezapour, Y. Orooji, The role of magnetite/graphene oxide nano-composite as a high-efficiency adsorbent for removal of phenazopyridine residues from water samples, an experimental/theoretical investigation, J. Mol. Liq. 298 (2020), https://doi.org/10.1016/j.molliq.2019.112040.
[8] M. Sheikholeslami, New computational approach for exergy and entropy analysis of nanofluid under the impact of Lorentz force through a porous media, Comput. Methods Appl. Mech. Eng. 344 (2019) 319–333.
[9] Z. Shamsadin-Azad, M.A. Taher, S. Cheraghi, H. Karimi-Maleh, J. Food Meas. Charact. 13 (2019) 1781–1787.
[10] M. Dehhaghi, M. Tabatabaei, M. Aghbashlo, H.K.S. Panahi, A.S. Nizami, A state-of-the-art review on the application of nanomaterials for enhancing biogas production, J. Environ. Manage. 251 (2019), https://doi.org/10.1016/j.jenvman.2019.109597.
[11] A.K. Geim, K.S. Novoselov, The rise of graphene, nanoscience and technology: a collection of reviews from nature journals, World Sci. (2010) 11–19.
[12] M.J. Allen, V.C. Tung, R.B. Kaner, Honeycomb carbon: a review of graphene, Chem. Rev. 110 (1) (2010) 132–145.
[13] T. Ohta, A. Bostwick, T. Seyller, K. Horn, E. Rotenberg, Controlling the electronic structure of bilayer graphene, Science 313 (5789) (2006) 951–954.
[14] D.H. Ho, Q. Sun, S.Y. Kim, J.T. Han, D.H. Kim, J.H. Cho, Stretchable and multimodal all graphene electronic skin, J. Adv. Mater. 28 (13) (2016) 2601–2608.
[15] W.J. Hyun, O.O. Park, B.D. Chin, Foldable graphene electronic circuits based on paper substrates, J. Adv. Mater. 25 (34) (2013) 4729–4734.
[16] G. Eda, G. Fanchini, M. Chhowalla, Large-area ultrathin films of reduced graphene oxide as a transparent and flexible electronic material, Nat. Nanotechnol. 3 (5) (2008) 270.
[17] X. Zhao, Q. Zhang, D. Chen, P.J.M. Lu, Enhanced mechanical properties of graphene-based poly (vinyl alcohol) composites, Macromoleucles 43 (5) (2010) 2357–2363.
[18] M. Fang, K. Wang, H. Lu, Y. Yang, S. Nutt, Covalent polymer functionalization of graphene nanosheets and mechanical properties of composites, J. Mater. Chem. 19 (38) (2009) 7098–7105.

[19] S. Stankovich, D.A. Dikin, G.H. Dommett, K.M. Kohlhaas, E.J. Zimney, E.A. Stach, R.D. Piner, S.T. Nguyen, R.S. Ruoff, Graphene-based composite materials, Nature 442 (7100) (2006) 282.

[20] Y. Zhou, Q. Bao, L.A.L. Tang, Y. Zhong, K.P. Loh, Hydrothermal dehydration for the "green" reduction of exfoliated graphene oxide to graphene and demonstration of tunable optical limiting properties, Chem. Mater. 21 (13) (2009) 2950–2956.

[21] M. Liu, X. Yin, E. Ulin-Avila, B. Geng, T. Zentgraf, L. Ju, F. Wang, X.J.N. Zhang, A graphene-based broadband optical modulator, Nature 474 (7349) (2011) 64.

[22] L. Wang, Y. Wang, T. Xu, H. Liao, C. Yao, Y. Liu, Z. Li, Z. Chen, D. Pan, L. Sun, M. Wu, Gram-scale synthesis of single-crystalline graphene quantum dots with superior optical properties, Nat. Commun. 5 (2014) 5357.

[23] L. Falkovsky, Optical properties of graphene, J. Phys. Conf. Ser., IOP Publ. (2008) 012004.

[24] Alexander A. Balandin, Thermal properties of graphene and nanostructured carbon materials, Nat. Mater 10 (8) (2011) 569–581, https://doi.org/10.1038/nmat3064.

[25] E. Pop, V. Varshney, A.K. Roy, Thermal properties of graphene: Fundamentals and applications, MRS Bull. 37 (12) (2012) 1273–1281.

[26] S.-Y. Yang, W.-N. Lin, Y.-L. Huang, H.-W. Tien, J.-Y. Wang, C.-C.M. Ma, S.-M. Li, Y.-S. Wang, Synergetic effects of graphene platelets and carbon nanotubes on the mechanical and thermal properties of epoxy composites, Carbon 49 (3) (2011) 793–803.

[27] A.K. Geim, Graphene, status and prospects, Sci. 324 (5934) (2009) 1530–1534.

[28] H. Chen, M.B. Müller, K.J. Gilmore, G.G. Wallace, D.J.A.M. Li, Mechanically strong, electrically conductive, and biocompatible graphene paper, Adv. Mat. 20 (18) (2008) 3557–3561.

[29] H. Shen, L. Zhang, M. Liu, Z.J.T. Zhang, Biomedical applications of graphene, Theranostics 2 (3) (2012) 283.

[30] H. Fan, L. Wang, K. Zhao, N. Li, Z. Shi, Z. Ge, Z.J.B. Jin, Fabrication, mechanical properties, and biocompatibility of graphene-reinforced chitosan composites, Biomacromolecules 11 (9) (2010) 2345–2351.

[31] A.B. Seabra, A.J. Paula, R. de Lima, O.L. Alves, N. Durán, Nanotoxicity of graphene and graphene oxide, Chem. Res. Toxicol. 27 (2) (2014) 159–168.

[32] Y. Zhang, T.-T. Tang, C. Girit, Z. Hao, M.C. Martin, A. Zettl, M.F. Crommie, Y.R. Shen, F.J.N. Wang, Direct observation of a widely tunable bandgap in bilayer graphene, Nat. 459 (7248) (2009) 820.

[33] E.V. Castro, K. Novoselov, S. Morozov, N. Peres, J.L. Dos Santos, J. Nilsson, F. Guinea, A. Geim, A.C. Neto, Biased bilayer graphene: semiconductor with a gap tunable by the electric field effect, Phys. Rev. Lett. 99 (21) (2007) 216802.

[34] R. Raccichini, A. Varzi, S. Passerini, B. Scrosati, The role of graphene for electrochemical energy storage, Nat. Mater. 14 (3) (2015) 271.

[35] Z.-S. Wu, G. Zhou, L.-C. Yin, W. Ren, F. Li, H.-M. Cheng, Graphene/metal oxide composite electrode materials for energy storage, Nano Energy 1 (1) (2012) 107–131.

[36] M.J.E. Pumera, E. Science, Graphene-based nanomaterials for energy storage, Energ. Environ. Sci. 4 (3) (2011) 668–674.

[37] F. Bonaccorso, L. Colombo, G. Yu, M. Stoller, V. Tozzini, A.C. Ferrari, R.S. Ruoff, V.J.S. Pellegrini, Graphene, related two-dimensional crystals, and hybrid systems for energy conversion and storage, Science 347 (6217) (2015) 1246501.

[38] Y. Xiao, X. Qu, K.W. Plaxco, A.J. Heeger, Label-free electrochemical detection of DNA in blood serum via target-induced resolution of an electrode-bound DNA pseudoknot, J. Am. Chem. Soc. 129 (39) (2007) 11896–11897.

[39] F.-Y. Kong, S.-X. Gu, W.-W. Li, T.-T. Chen, Q. Xu, W.J.B. Wang, Bioelectronics, A paper disk equipped with graphene/polyaniline/Au nanoparticles/glucose oxidase biocomposite modified screen-printed electrode: toward whole blood glucose determination, Biosens. Bioelecron. 56 (2014) 77–82.

[40] Y. Song, Y.-Y. Huang, X. Liu, X. Zhang, M. Ferrari, L. Qin, Point-of-care technologies for molecular diagnostics using a drop of blood, Trends Biotechnol. 32 (3) (2014) 132–139.

[41] P. Bollella, G. Fusco, D. Stevar, L. Gorton, R. Ludwig, S. Ma, H. Boer, A. Koivula, C. Tortolini, G.J.S. Favero, A.B. Chemical, A glucose/oxygen enzymatic fuel cell based on gold nanoparticles modified graphene screen-printed electrode proof-of-concept in human saliva, Sens. Actuat. B-Chem. 256 (2018) 921–930.

[42] D. Ye, G. Liang, H. Li, J. Luo, S. Zhang, H. Chen, J.J.T. Kong, A novel nonenzymatic sensor based on CuO nanoneedle/graphene/carbon nanofiber modified electrode for probing glucose in saliva, Talanta 116 (2013) 223–230.

[43] J. Ping, J. Wu, Y. Wang, Y.J.B. Ying, Bioelectronics, simultaneous determination of ascorbic acid, dopamine and uric acid using high-performance screen-printed graphene electrode, Biosens. Bioelecron. 34 (1) (2012) 70–76.

[44] P. Kanyong, S. Rawlinson, J.J.C. Davis, A voltammetric sensor based on chemically reduced graphene oxide-modified screen-printed carbon electrode for the simultaneous analysis of uric acid, ascorbic acid and dopamine, Chemosensors 4 (4) (2016) 25.

[45] H. Karimi-Maleh, O.A. Arotiba, Simultaneous determination of cholesterol, ascorbic acid and uric acid as three essential biological compounds at a carbon paste electrode modified with copper oxide decorated reduced graphene oxide nanocomposite and ionic liquid, J. Colloid Interf. Sci. 560 (2020.) 208–212.

[46] H. Karimi-Maleh, F. Karimi, M. Alizadeh, A.L. Sanati, Electrochemical sensors, a bright future in the fabrication of portable kits in analytical systems, Chem. Record (2019), https://doi.org/10.1002/tcr.201900092.

[47] D. Durgalakshmi, R.A. Rakkesh, J. Mohanraj, Graphene–Metal–Organic Framework-Modified Electrochemical Sensors, in: Graphene-Based Electrochemical Sensors for Biomolecules, Elsevier, 2019, pp. 275–296.

[48] X. Dong, Y. Shi, W. Huang, P. Chen, L.J. Li, Electrical detection of DNA hybridization with single-base specificity using transistors based on CVD-grown graphene sheets, Adv. Mater. 22 (14) (2010) 1649–1653.

[49] Q. He, H.G. Sudibya, Z. Yin, S. Wu, H. Li, F. Boey, W. Huang, P. Chen, H. Zhang, Centimeter-long and large-scale micropatterns of reduced graphene oxide films: fabrication and sensing applications, ACS Nano 4 (6) (2010) 3201–3208.

[50] J.R. Windmiller, J.J.E. Wang, Wearable electrochemical sensors and biosensors: a review, Electroanalysis 25 (1) (2013) 29–46.

[51] J. Barton, M.B.G. García, D.H. Santos, P. Fanjul-Bolado, A. Ribotti, M. McCaul, D. Diamond, P. Magni, Screen-printed electrodes for environmental monitoring of heavy metal ions: a review, Microchim. Acta 183 (2) (2016) 503–517.

[52] A.K. Sundramoorthy, S. Gunasekaran, Applications of graphene in quality assurance and safety of food, Trend. Anal. Chem. 60 (2014) 36–53.

[53] L. Rotariu, F. Lagarde, N. Jaffrezic-Renault, C. Bala, Electrochemical biosensors for fast detection of food contaminants–trends and perspective, TrAC Trends Anal. Chem. 79 (2016) 80–87.

[54] H. Tao, M.A. Brenckle, M. Yang, J. Zhang, M. Liu, S.M. Siebert, R.D. Averitt, M.S. Mannoor, M.C. McAlpine, J.A. Rogers, D.L. Kaplan, Silk-based conformal, adhesive, edible food sensors, Adv. Mater. 24 (8) (2012) 1067–1072.

[55] R.K. Pal, A.A. Farghaly, C. Wang, M.M. Collinson, S.C. Kundu, V.K. Yadavalli, Bioelectronics, conducting polymer-silk biocomposites for flexible and biodegradable electrochemical sensors, Biosens. Bioelectron. 81 (2016) 294–302.

[56] H. Kudo, T. Sawada, E. Kazawa, H. Yoshida, Y. Iwasaki, K.J.B. Mitsubayashi, Bioelectronics, a flexible and wearable glucose sensor based on functional polymers with Soft-MEMS techniques, Biosens. Bioelectron. 22 (4) (2006) 558–562.

[57] S. Wang, T. Chinnasamy, M.A. Lifson, F. Inci, U. Demirci, Flexible substrate-based devices for point-of-care diagnostics, Trends Biotechnol. 34 (11) (2016) 909–921.

[58] K. Yamada, T.G. Henares, K. Suzuki, D. Citterio, Paper-based inkjet-printed microfluidic analytical devices, Angew. Chem. Int. Ed. Engl. 54 (18) (2015) 5294–5310.

[59] A. Erlenkötter, M. Kottbus, G.-C. Chemnitius, Flexible amperometric transducers for biosensors based on a screen printed three electrode system, J. Electroanal. Chem. 481 (1) (2000) 82–94.

[60] F.J. Pavinatto, C.W. Paschoal, A.C. Arias, Bioelectronics, Printed and flexible biosensor for antioxidants using interdigitated ink-jetted electrodes and gravure-deposited active layer, Biosens. Bioelectron. 67 (2015) 553–559.

[61] M. Magliulo, M. Mulla, M. Singh, E. Macchia, A. Tiwari, L. Torsi, K.J. Manoli, Printable and flexible electronics: from TFTs to bioelectronic devices, J. Mater. Chem. C 3 (48) (2015) 12347–12363.

[62] V. Dua, S.P. Surwade, S. Ammu, S.R. Agnihotra, S. Jain, K.E. Roberts, S. Park, R.S. Ruoff, S. Manohar, All-organic vapor sensor using inkjet-printed reduced graphene oxide, Angew. Chem. Int. Ed. Engl. 49 (12) (2010) 2154–2157.

[63] M. Ligaj, M. Tichoniuk, D. Gwiazdowska, M. Filipiak, Electrochemical DNA biosensor for the detection of pathogenic bacteria aeromonas hydrophila, Elecytrochim. Acta. 128 (2014) 67–74.

[64] J.J. Gau, E.H. Lan, B. Dunn, C.M. Ho, J.C. Woo, A MEMS based amperometric detector for E. coli bacteria using self-assembled monolayers, Biosens. Bioelectron. 16 (9–12) (2001) 745–755.

[65] N. Sanvicens, C. Pastells, N. Pascual, M.P. Marco, Nanoparticle-based biosensors for detection of pathogenic bacteria, TrAC Trends Analyt. Chem. 28 (11) (2009) 1243–1252.

[66] A. Hájková, J. Barek, V.J.B. Vyskočil, Electrochemical DNA biosensor for detection of DNA damage induced by hydroxyl radicals, Bioelectrochemistry 116 (2017) 1–9.

[67] H. Karimi-Maleh, F. Tahernejad-Javazmi, N. Atar, M.L. Yola, V.K. Gupta, A.A. Ensafi, A novel DNA biosensor based on a pencil graphite electrode modified with polypyrrole/functionalized multiwalled carbon nanotubes for determination of 6-mercaptopurine anticancer drug, Indust. Eng. Chem. Res. 54 (14) (2015) 3634–3639.

[68] H.-S. Wang, H.-X. Ju, H.-Y. Chen, Simultaneous determination of guanine and adenine in DNA using an electrochemically pretreated glassy carbon electrode, Anal. Chim. Acta 461 (2) (2002) 243–250.

[69] H. Liu, G. Wang, D. Chen, W. Zhang, C. Li, B.J.S. Fang, A.B. Chemical, Fabrication of polythionine/NPAu/MWNTs modified electrode for simultaneous determination of adenine and guanine in DNA, Sensor Actuat. B-Chem. 128 (2) (2008) 414–421.

[70] H. Sahoo, Fluorescent labeling techniques in biomolecules: a flashback, RSC Adv. 2 (18) (2012) 7017–7029.

[71] J. Labuda, R. Ovádeková, J. Galandová, DNA-based biosensor for the detection of strong damage to DNA by the quinazoline derivative as a potential anticancer agent, Microchim. Acta 164 (3–4) (2009) 371–377.

[72] J. Ping, S. Ru, X. Luo, K. Fan, J. Wu, Y. Ying, Direct electrochemistry of double strand DNA on ionic liquid modified screen-printed graphite electrode, Electrochim. Acta 56 (11) (2011) 4154–4158.

[73] L. Hlavata, K. Benikova, V. Vyskocil, J. Labuda, Evaluation of damage to DNA induced by UV-C radiation and chemical agents using electrochemical biosensor based on low molecular weight DNA and screen-printed carbon electrode, Electrochim. Acta 71 (2012) 134–139.

[74] Z. Zhu, X. Li, Y. Zeng, W.J.B. Sun, Bioelectronics, Ordered mesoporous carbon modified carbon ionic liquid electrode for the electrochemical detection of double-stranded DNA, Biosens. Bioelectron. 25 (10) (2010) 2313–2317.
[75] D. Wang, B. Huang, J. Liu, X. Guo, G. Abudukeyoumu, Y. Zhang, B.-C. Ye, Y.J.B. Li, Bioelectronics, A novel electrochemical sensor based on Cu@ Ni/MWCNTs nanocomposite for simultaneous determination of guanine and adenine, Biosens. Bioelectron. 102 (2018) 389–395.
[76] M. Genovese, J. Jiang, K. Lian, N.J. Holm, High capacitive performance of exfoliated biochar nanosheets from biomass waste corn cob, J. Mater. Chem. 3 (6) (2015) 2903–2913.
[77] J. Mohanraj, D. Durgalakshmi, S. Balakumar, P. Aruna, S. Ganesan, S. Rajendran, M.J. Naushad, Low, cost and quick time absorption of organic dye pollutants under ambient condition using partially exfoliated graphite, J. Water Process Eng. (2019) 101078.
[78] D.C. Marcano, D.V. Kosynkin, J.M. Berlin, A. Sinitskii, Z. Sun, A. Slesarev, L.B. Alemany, W. Lu, J.M. Tour, Improved synthesis of graphene oxide, ACS Nano 4 (8) (2010) 4806–4814.
[79] Y. Zhu, S. Murali, W. Cai, X. Li, J.W. Suk, J.R. Potts, R.S. Ruoff, Graphene and graphene oxide: synthesis, properties, and applications, Adv. Mater. 22 (35) (2010) 3906–3924.
[80] S.J. Chae, F. Güneş, K.K. Kim, E.S. Kim, G.H. Han, S.M. Kim, H.J. Shin, S.M. Yoon, J.Y. Choi, M.H. Park, Synthesis of large-area graphene layers on poly-nickel substrate by chemical vapor deposition: wrinkle formation, Adv. Mater. 21 (22) (2009) 2328–2333.
[81] S. Stankovich, D.A. Dikin, R.D. Piner, K.A. Kohlhaas, A. Kleinhammes, Y. Jia, Y. Wu, S.T. Nguyen, R.S. Ruoff, Synthesis of graphene-based nanosheets via chemical reduction of exfoliated graphite oxide, Carbon 45 (7) (2007) 1558–1565.
[82] H.-L. Guo, X.-F. Wang, Q.-Y. Qian, F.-B. Wang, X.-H. Xia, A green approach to the synthesis of graphene nanosheets, ACS Nano 3 (9) (2009) 2653–2659.
[83] H. Karimi-Maleh, M. Shafieizadeh, M.A. Taher, F. Opoku, E.M. Kiarii, P.P. Govender, S. Ranjbari, M. Rezapour, Y.J. Orooji, The role of magnetite/graphene oxide nano-composite as a high-efficiency adsorbent for removal of phenazopyridine residues from water samples, an experimental/theoretical investigation, J. Mol. Liq. 112040 (2019).
[84] K. Parvez, Z.-S. Wu, R. Li, X. Liu, R. Graf, X. Feng, K.J. Müllen, Exfoliation of graphite into graphene in aqueous solutions of inorganic salts, J. Am. Chem. Soc. 136 (16) (2014) 6083–6091.
[85] J. Lu, J.-X. Yang, J. Wang, A. Lim, S. Wang, K. Loh, One-pot synthesis of fluorescent carbon nanoribbons, nanoparticles, and graphene by the exfoliation of graphite in ionic liquids, ACS Nano 3 (8) (2009) 2367–2375.
[86] J. Liu, H. Yang, S.G. Zhen, C.K. Poh, A. Chaurasia, J. Luo, X. Wu, E.K.L. Yeow, N.G. Sahoo, J. Lin, Z. Shen, A green approach to the synthesis of high-quality graphene oxide flakes via electrochemical exfoliation of pencil core, RSC Adv. 3 (29) (2013) 11745–11750.
[87] K.S. Novoselov, V.I. Fal'ko, L. Colombo, P.R. Gellert, M.G. Schwab, K. Kim, A roadmap for graphene, Nature 490 (7419) (2012) 192–200, https://doi.org/10.1038/nature11458.
[88] Z. Sun, Z. Yan, J. Yao, E. Beitler, Y. Zhu, J.M.J.N. Tour, Growth of graphene from solid carbon sources, Nat. 468 (7323) (2010) 549.
[89] S. Bae, H. Kim, Y. Lee, X. Xu, J.-S. Park, Y. Zheng, J. Balakrishnan, T. Lei, H.R. Kim, Y. Song, Roll-to-roll production of 30-inch graphene films for transparent electrodes, Nat. Nanotechnol. 5 (8) (2010) 574.
[90] Xiaolin Li, Guangyu Zhang, Xuedong Bai, Xiaoming Sun, Xinran Wang, Enge Wang, Hongjie Dai, Highly conducting graphene sheets and Langmuir–Blodgett films, Nat. Nanotech. 3 (9) (2008) 538–542, https://doi.org/10.1038/nnano.2008.210.
[91] J. Chen, B. Yao, C. Li, G.J.C. Shi, An improved Hummers method for eco-friendly synthesis of graphene oxide, Carbon 64 (2013) 225–229.
[92] J. Chen, Y. Li, L. Huang, C. Li, G.J.C. Shi, High-yield preparation of graphene oxide from small graphite flakes via an improved Hummers method with a simple purification process, Carbon 81 (2015) 826–834.
[93] C.-H. Chuang, C.-Y. Su, K.-T. Hsu, C.-H. Chen, C.-H. Huang, C.-W. Chu, W.-R. Liu, A green, simple and cost-effective approach to synthesize high quality graphene by electrochemical exfoliation via process optimization, RSC Adv. 5 (67) (2015) 54762–54768.
[94] K. Chen, D. Xue, S. Komarneni, Nanoclay assisted electrochemical exfoliation of pencil core to high conductive graphene thin-film electrode, J. Ccolloid Interf. Sci. 487 (2017) 156–161.
[95] M. Yi, Z. Shen, X. Zhang, S.J.J.o.P.D.A.P. Ma, Achieving concentrated graphene dispersions in water/acetone mixtures by the strategy of tailoring Hansen solubility parameters, J. Phys. D. Appl. Phys. 46(2) (2012) 025301.
[96] I. Kumar, A. Khare, Multi-and few-layer graphene on insulating substrate via pulsed laser deposition technique, Appl. Surg. Sci. 317 (2014) 1004–1009.
[97] F. Miao, S. Majee, M. Song, J. Zhao, S.-L. Zhang, Z.-B. Zhang, Inkjet printing of electrochemically-exfoliated graphene nano-platelets, Synth. Met. 220 (2016) 318–322.
[98] A.C. Ferrari, J. Meyer, V. Scardaci, C. Casiraghi, M. Lazzeri, F. Mauri, S. Piscanec, D. Jiang, K. Novoselov, S.J. Roth, Raman spectrum of graphene and graphene layers, Phys. Rev. Lett. 97 (18) (2006) 187401.
[99] A. Kaur, J. Kaur, R. Singh, Green, exfoliation of graphene nanosheets based on freezing induced volumetric expansion of carbonated water, Mater. Res. Express 5(8) (2018) 085601.
[100] A. Primo, P. Atienzar, E. Sanchez, J.M. Delgado, H.J.C.c. García, From biomass wastes to large-area, high-quality, N-doped graphene: catalyst-free carbonization of chitosan coatings on arbitrary substrates, Chem Comm. 48 (74) (2012) 9254-9256.
[101] Y. Fan, K.-J. Huang, D.-J. Niu, C.-P. Yang, Q.-S. Jing, TiO_2-graphene nanocomposite for electrochemical sensing of adenine and guanine, Electrochmica Acta 56 (12) (2011) 4685–4690.
[102] S.R. Balakrishnan, U. Hashim, G. Letchumanan, M. Kashif, A. Ruslinda, W. Liu, P. Veeradasan, R.H. Prasad, K. Foo, P.J.S. Poopalan, A.A. Physical, Development of highly sensitive polysilicon nanogap with APTES/GOx based lab-on-chip biosensor to determine low levels of salivary glucose, Sens. Actuat. A Phys. 220 (2014) 101–111.
[103] E.N. Primo, F.A. Gutierrez, M.D. Rubianes, G. Rivas, Bamboo-like multiwalled carbon nanotubes dispersed in double stranded calf-thymus DNA as a new analytical platform for building layer-by-layer based biosensors, Electrochmica Acta 182 (2015) 391–397.
[104] J.H. Kim, W.S. Chang, D. Kim, J.R. Yang, J.T. Han, G.W. Lee, J.T. Kim, S.K.J.A.M. Seol, 3D printing of reduced graphene oxide nanowires, Adv. Mater. 27(1) (2015) 157-161.
[105] A.E. Jakus, E.B. Secor, A.L. Rutz, S.W. Jordan, M.C. Hersam, R. Shah, Three-dimensional printing of high-content graphene scaffolds for electronic and biomedical applications, ACS Nano 9 (4) (2015) 4636–4648.
[106] C. Zhu, T.Y.-J. Han, E.B. Duoss, A.M. Golobic, J.D. Kuntz, C.M. Spadaccini, M.A.J. N.c. Worsley, Highly compressible 3D periodic graphene aerogel microlattices, Nat. Commun. 6 (2015) 6962.
[107] E. García-Tuñon, S. Barg, J. Franco, R. Bell, S. Eslava, E. D'Elia, R.C. Maher, F. Guitian, E. Saiz, Printing in three dimensions with graphene, Adv. Mater. 27 (10) (2015) 1688–1693.
[108] W. Li, F. Li, H. Li, M. Su, M. Gao, Y. Li, D. Su, X. Zhang, Y. Song, Flexible circuits and soft actuators by printing assembly of graphene, ACS Appl. Mater. Interf. 8 (19) (2016) 12369–12376.